Effect of Motion on Thallium-201 SPECT Studies: A Simulation and Clinical Study

Florence M. Prigent, Mark Hyun, Daniel S. Berman and Alan Rozanski*

Departments of Medicine (Division of Cardiology) and Nuclear Medicine, Cedars-Sinai Medical Center; and the Department of Medicine, UCLA School of Medicine, Los Angeles, California

Although patient motion on ^{201}Tl SPECT studies has been reported as a source of artifacts, systematic studies on motion patterns and resultant artifacts are lacking. Accordingly, we simulated 74 motion patterns upon a normal study. The tomograms were assessed for presence of defects: The "motion pixel area index" ranged from 1 to 83; 26 of 30 (87%) simulations with an index ≥21 had defects, whereas 38 of 44 (86%) simulations with an index <21 were normal. Defect location was dependent on motion direction; defect intensity was dependent on its magnitude and timing. Review of data acquisition in 164 recent normal patient studies revealed motion in 42 (26%). Motion was generally minimal and caused defects in only seven (4%). Thus, mild motion is unlikely to produce defects. In our laboratory, motion is now an infrequent source of artifacts; severe motion produces recognizable patterns that depend on its direction, magnitude and timing.

J Nucl Med 1993; 34:1845–1850

The occurrence of patient motion during acquisition of SPECT ^{201}Tl studies is well recognized as a potential source of false-positive studies, due to resultant artifacts in the reconstructed tomograms (*1–3*). But the impact of patient motion on test specificity is not well known due to a lack of knowledge regarding the frequency of patient motion in current clinical laboratories. Furthermore, relatively little is known regarding the magnitude and pattern of patient motion required to produce artifactual defects. Knowledge of motion patterns and resultant artifacts could help in interpreting studies involving suspected motion, thereby improving the overall specificity of stress-redistribution ^{201}Tl SPECT imaging for the detection of coronary artery disease. To address these issues, we undertook the following study involving three goals. First, we employed a simulation study to assess how different motion patterns affect the presence, location and intensity of artifactual defects on reconstructed tomograms. Second, we determined if the scintigraphic patterns encountered by a given simulation matched the scintigraphic patterns encountered in routine clinical studies in which similar types of motion were observed. Third, we assessed the frequency and magnitude of patient motion and its impact on test specificity in a population of normal patients who were tested in our laboratory.

Received July 20, 1992; revision accepted June 25, 1993.

For correspondence or reprints contact: Florence Prigent, MD, 1915 Brickell Ave., #C813, Miami, FL 33129.

*Presently at St. Luke's/Roosevelt Medical Center, New York, NY.

METHODS

Simulation Study

A representative normal stress-redistribution SPECT ^{201}Tl study was selected from our laboratory database. The study was that of a 40-yr-old male with nonanginal chest pain and a normal treadmill electrocardiographic response to stress. The patient's calculated Bayesian likelihood of coronary artery disease was low (<5%) (*4*). No motion was present on the initial projections and the patient's study was normal by both visual and quantitative analysis. We used the postexercise study to create 74 different motion simulations by moving one or multiples of the initial projections for a various number of integral pixels, to mimic motion patterns usually occurring in our laboratory (Table 1).

For each simulation, we recorded the following parameters: (1) the number of frames moved; (2) the maximal shift (in integral pixels); (3) the direction of motion (upward, downward, lateral); and (4) the timing of motion relative to data acquisition. The 74 motion simulation patterns were divided into four basic types: (1) "bounce" was brief motion, observed in ≤3 consecutive frames, deviating from 1 to 4 pixels from the baseline (i.e., the horizontal axis delineated by the rotating projections); (2) "shift" was defined as >3 consecutive frames deviating from the baseline in a similar fashion, that either did not return to baseline (single shift) or returned to baseline (double shift); (3) "complex motion" combined bounces and shifts; and (4) "lateral motion" was created by moving the frames horizontally rather than vertically.

Once the simulations were created, the studies were reconstructed in a standard fashion. The different motion patterns were then compared to the extent of visually and quantitatively determined defects on the tomograms.

To define motion extent, a motion pixel area (MOPA) index was created, defined as the total pixel deviation in each study. For instance, if three frames were moved two pixels each, the MOPA index was equal to six. To assess the effect of motion amplitude, simulations of motion with similar direction and timing, but different amplitude were created. To assess the effect of motion direction, simulations of motion of similar amplitude and timing, but different direction, were created. To assess the effect of the timing of motion, the initial projections were divided into five zones of 6–7 frames each; i.e., Zone 1 corresponded to Frames 1–6; Zone 2 to Frames 7–12; Zone 3 to Frames 13–18; Zone 4 to Frames 19–25; and Zone 5 to Frames 26–32. Motion of similar

TABLE 1
Motion Simulations Used In the Study

	Direction		
	Up	Down	Up and down
Vertical motion: (63)			
Single bounce: 26	10	16	0
Multiple bounces: 2	2	0	0
Single shift: 11	5	6	0
Double shifts: 8	4	4	0
Complex motion: 16	10	5	1
Lateral motion: 9	Right	Left	
Bounces: 5	1	4	
Shifts: 4	1	3	
No motion created: (2)			
Total: (74)			

amplitude and direction was created in the different zones. Image artifacts other than defects were also recorded.

Clinical Study

We performed a retrospective analysis on the presence and characteristics of motion in two groups of patients. The normal patient population was comprised of 164 patients who underwent stress redistribution ^{201}Tl SPECT in our laboratory between January 1987 and December 1989 and had ≤5% likelihood of coronary artery disease, based on Bayesian analysis of patient age, gender, risk factors, symptoms classification and the results of exercise electrocardiography (*4*). These normals were randomly selected from our database. The clinical postexercise studies were assessed for the presence and characteristics of observed motion by two blinded observers, by examining the composite image of the added projections on a static mode and by viewing all of the projections in a movie display format. The deviation of the point source from the horizontal line on both the composite image and on the movie display format was also recorded. The normal patient group was used to assess the frequency of patient motion in a normal patient population. A separate patient motion group was comprised of nine patients who were selected because of known motion during the acquisition of their exercise SPECT study. This group was used to assess if the motion patterns encountered in clinical studies matched the defects patterns created in the simulation studies for identical types of motion.

Exercise and Imaging Protocol

All patients underwent a symptom-limited treadmill exercise using the standard Bruce protocol. A dose of 3–4 mCi of ^{201}Tl was injected near peak exercise and exercise was continued for an additional minute. SPECT imaging was performed at 15 min and 4 hr following injection, according to our previously described technique (*5*) consisting of 32 (40 sec) projections over 180°. The scintillation cameras were equipped with a 0.25-in. thick NAI(Tl) crystal and a low-energy, all-purpose parallel hole collimator. The pixel size was 0.64 cm × 0.64 cm. All tomographic data was corrected for center of rotation. Uniformity correction was done with a Cobalt-57 flood source for 30 million counts. At the time of acquisition, two ^{201}Tl point sources were placed immediately above and below the myocardial area to help in detecting motion (*1*).

Image Analysis (Simulation and Clinical Studies)

After smoothing of the SPECT projections, horizontal long-axis, short-axis and vertical long-axis tomograms were obtained. They were visually interpreted blindly by two experienced observers for the intensity and location of defects and were divided into 20 segments (Fig. 1). Thallium-201 activity in each segment was scored on a four-point scoring system. The SPECT score was defined as the sum of segments with moderately or severely decreased tracer activity (i.e., sum of segments with scores ≥2). At least two myocardial segments had to have scores ≥2 for the study to be considered abnormal. All images were also assessed for the presence of scintigraphic artifacts: For each simulation, each artifact was graded as absent (score = 0), mild (score = 1) or definite (score = 2). The total artifact score was recorded for each study.

For quantification, maximum count circumferential profiles were generated and plotted into polar maps which were divided into vascular territories. These have been defined from studies of patients with single-vessel disease in which the territories had ≥80% likelihood of being associated with a stenosis in the individual coronary artery. With this display, a study is considered abnormal when the percentage of abnormal points in at least one vascular territory is above or equal to a threshold number which is specific for each of the three territories. While we also assessed the defect size (as a percentage) for the entire left ventricle, no criteria for abnormality has been adapted for this parameter, as we found it less specific than assessing individual coronary territories.

Statistical Analysis

The SPECT scores and quantitative defect size were expressed as mean ± s.d. Statistical analysis were not performed on simulation results that involved arbitrary distributions.

RESULTS

Simulation Study

Motion Magnitude. The relation between the visual SPECT score and the magnitude of motion, expressed in MOPA units, is illustrated in Figure 2. A threshold of 21 MOPA units best separated the normal from abnormal studies. Thirty-eight (86%) of the 44 studies with a MOPA index <21 were normal, whereas 26 (87%) of the 30 studies with a MOPA index ≥21 were considered abnormal. The SPECT score was very low till a MOPA index of 21, indicating that mild degrees of motion usually do not produce defects. Among the abnormal studies, however, the extent of perfusion abnormalities was not linearly correlated with the MOPA index.

The same threshold of 21 MOPA units was found for quantitative analysis (Fig. 3). All studies with a MOPA index <21 were quantitatively normal, whereas 17 (57%) of the 30 studies with a MOPA index ≥21 were found to have ≥3% hypoperfused myocardium. Of these 17 studies, eight

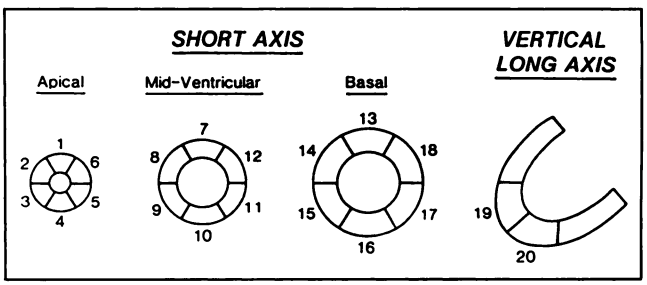

FIGURE 1. Scoring system for visual analysis. Each segment is scored on a four-point scale: 0 = normal, 1 = mild decrease, 2 = moderate decrease and 3 = severe decrease in ^{201}Tl activity.

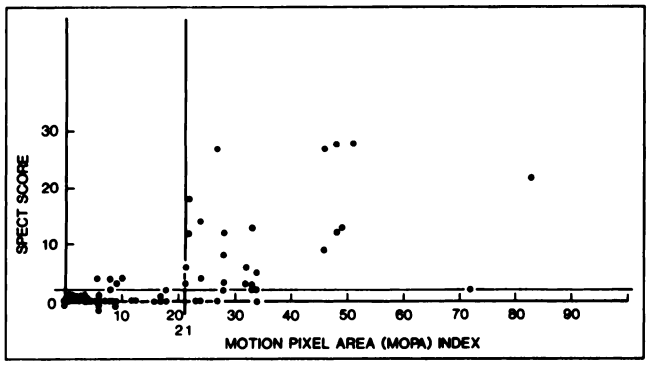

FIGURE 2. Relationship between the magnitude of motion (MOPA index) and the magnitude of abnormalities (Visual SPECT score).

were abnormal by quantitative analysis (i.e., the criteria for abnormality was exceeded in at least one specific vessel territory), in the nine others, some of the abnormal points fell into the border zones and the number of abnormal points falling into the vascular territories were insufficient to meet the criteria for abnormality.

Magnitude of Shift. Figure 4 illustrates the added projections, samples of the short-axis tomograms and the polar maps of three representative motion simulations in which the last 16 projections were moved downward by either one, two or three pixels. With a one-pixel deviation, there was no perfusion defect. With a two-pixel deviation, there was a mild anteroseptal defect (arrow on tomogram and black area on the polar map). With a three-pixel deviation, there were definite defects in the antero-septal and inferior walls.

When considering all simulations, none of the 14 simulations that had a maximal shift of one pixel had a significant abnormality. This was true regardless of the number of frames moved, the direction or the timing of motion. In the 28 simulations with a two-pixel shift, the mean visual score was 3.0 ± 4.5 and the mean quantitative score was

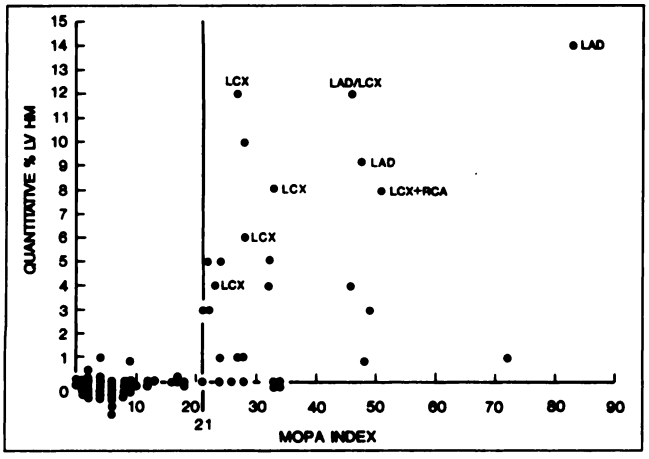

FIGURE 3. Relationship between the magnitude of motion (MOPA index) and the quantitative % defect size. The symbols LAD (left anterior descending), LCX (left circumflex artery) and RCA (right coronary artery) indicate that the studies are abnormal by quantitative analysis in the corresponding vessel(s).

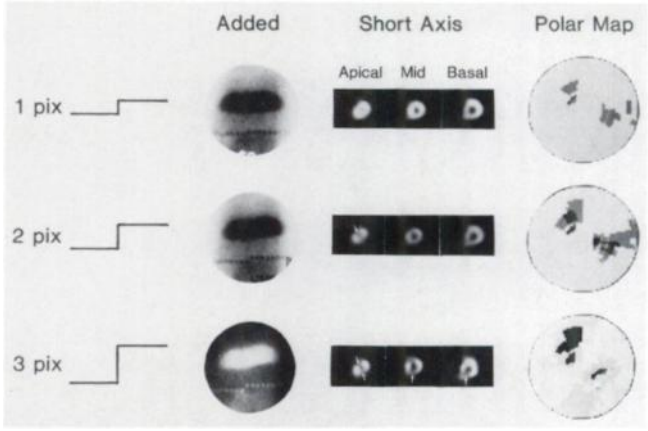

FIGURE 4. Added images, samples of short-axis tomograms and polar maps in three downward motion simulations. The same frames are moved, but the magnitude of shift varies: from 1 pixel (top) to 3 pixels (bottom). On the polar map, the circumferential profile points falling below normal are depicted according to the magnitude of defect abnormality. The magnitude of defects is presented according to a gray scale, with definite abnormalities depicted in dark gray and black.

1% ± 2%. In the 30 simulations with a three-pixel or four-pixel shift, the mean visual score was 7.5 ± 9.5 and the mean quantitative score was 3% ± 4%. Thus, the greater the amount of shift, the greater the extent of artifactual defect.

Vertical Motion. The scintigraphic findings in the simulation with vertical motion are summarized in Table 2. Eleven of the 31 studies with downward motion had defects which were all located in the anteroseptal wall and were associated in three cases with inferior wall defects; 16 of the 31 studies with upward motion had defects, 13 of which were located in the anterolateral wall and six of them in the inferior wall. In three cases of severe upward motion, these defects were associated with a septal defect in the most apical short-axis slice. The one simulation with bidirectionnal motion, that is both upward and downward with regard to the baseline, showed an inferior wall defect. Typical defects produced by upward or downward motion are shown in Figure 5.

TABLE 2
Dependence of Defect Location on Motion Direction in 63 Simulation Studies of Vertical Motion

		Location of defects					
Direction	No.	Ant-lat	Ant-lat and Inf	Inf	Ant-Sept and Inf	Ant-Sept	None
Up	31	3	10*	3	0	0	15
Do	31	0	0	0	3	8	20
Bi	1	0	0	1	0	0	0

*In three cases of severe motion, there was also decreased septal activity in the most apical short-axis slice.

Ant-lat = antero-lateral; Ant-sept = antero-septal; Bi = bi-directional; Do = downward motion; Inf = inferior; and Up = upward motion.

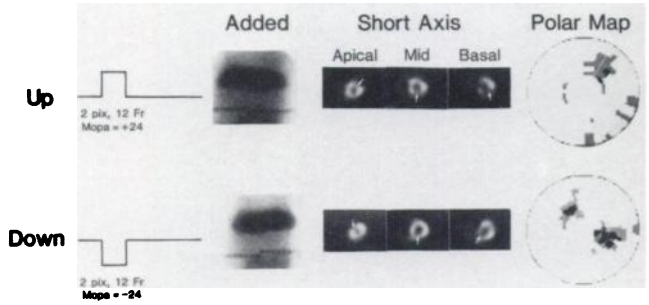

FIGURE 5. Identical motion simulations, except for the direction of motion: frames 16–27 have been moved two pixels either upward (top) or downward (bottom).

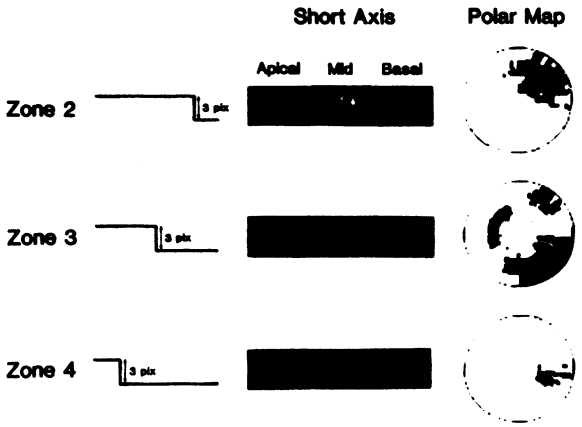

FIGURE 6. Motion simulation with similar direction and magnitude of shift, but in which the timing of motion differed.

Timing of Motion. Figure 6 illustrates the tomographic findings in three simulations of upward motion in which the timing of motion varied: On the top row, motion was created "early," beginning at the ninth frame, with the subsequent 24 frames (9–32) moved by three pixels. On the middle row, motion was created at midacquisition, and 16 frames (16–32) were moved three pixels. On the bottom row, motion was created in the last eight frames (24–32). There were extensive anterolateral and inferior wall defects in case of midacquisition motion, associated with hot spots in the lateral wall and decreased septal activity in the most apical slice. There was a mild anterolateral wall defect with early motion. The study with late motion was normal.

In all simulations with an inferior wall defect (n = 18), the motion involved the middle frames, and there was at least a 2-pixel deviation. In simulations with no inferior wall defect, motion involved the middle frames in only 27% of the 56 associated simulations. Thus, motion occurring in the middle of acquisition resulted in more extensive defects than motion occurring at the beginning or end of acquisition. Motion occurring at the end of acquisition was particularly unlikely to result in extensive defects.

Bounce. With single bounce, no defects were present except for the two simulations in which the middle frames (15–17) were moved up by two pixels (resulting in a small inferior wall defect) or three pixels (resulting in a small inferior and anterior wall defect). In the two simulations with multiple bounces, for which one bounce involved the middle frames, a small inferior wall defect was visually present in both cases.

Lateral Motion. Lateral bounce did not produce perfusion defects. Lateral shifts of two pixels produced no perfusion defects but did produce an early septal drop-off and increased right ventricular activity. Lateral motion of three pixels produced lateral wall defects.

Artifacts. Beside the induction of defects, six types of scintigraphic artifacts were identified (Fig. 7): tailing of activity into the background; distortion of the basal slices; dislocation of the tomograms; hot spots; and with lateral motion, early septal drop-off and increased right ventricular activity could be observed. Using the prior threshold of 21 MOPA units, 41/44 (93%) of the studies with a MOPA index <21 had an artifact score of <2, whereas 25/30 (83%) of the studies with a MOPA index ≥21 had an artifact score of ≥2.

Clinical Study

Of the 164 patients of the normal group, 42 (26%) were found to have visually detectable motion on their rotating stress images. The types of motion encountered are summarized in Table 3. However, of these 42 patients, only seven had defects that could be attributed to motion. In the motion group, there were five false-positive studies which were judged to be unrelated to motion. One study with upward creep had a lateral defect which was clearly related to breast attenuation. Four poststress studies with bounce had inferior wall defects which were also present on the redistribution images, with no associated patient motion during redistribution imaging. Of the 122 patients with no motion on their rotating images, only one (1%) was found to have a defect pattern suggestive of motion.

Table 4 summarizes the clinical findings and the charac-

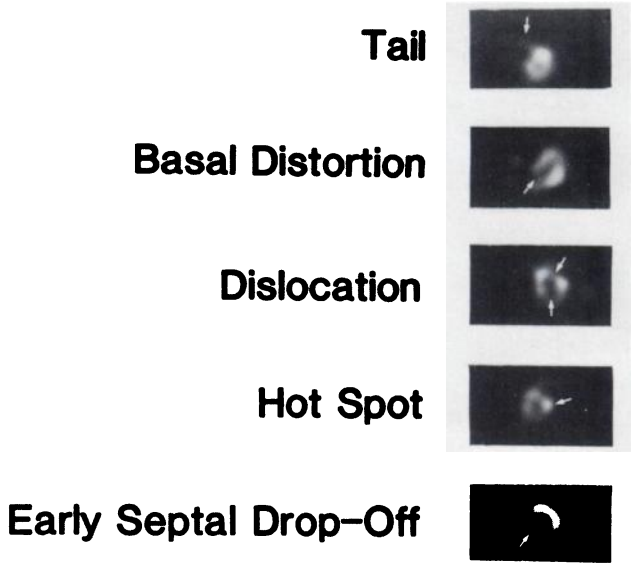

FIGURE 7. Artifacts commonly encountered in cases of severe motion.

teristics of motion in these seven patients along with those of the motion group. Also shown are the defects which were predicted from the motion pattern, as well as the actual defects: in 13 patients, the observed defects matched the defects predicted from the simulations studies with similar types of motion. In two patients (12 and 16), the actual studies were normal while inferior defects were predicted. In Patient 1, an anteroseptal defect was predicted, while anteroseptal and inferior defects were actually present.

DISCUSSION

Various studies have indicated the superiority of SPECT thallium imaging over planar imaging for quantifying the magnitude of myocardial ischemia (*6–8*). Despite its inherent advantages, SPECT imaging is technically more exacting than planar imaging, and thus, there is more potential for false-positive responses due to the technical factors associated with SPECT imaging. Patient motion is one important cause for false-positive scintigraphic patterns with SPECT imaging (*1–3*), but the magnitude of motion required to induce motion artifacts is debated. Thus, this study was designed to assess the relationship between the presence, magnitude and different patterns of motion and the resultant abnormal patterns found on reconstructed tomograms. First, we employed a simulation study of patient motion, because the number of studies with significant motion in normal patients was too small to assess the relation between the various types of patient motion and the resultant scintigraphic patterns on tomograms. Using 74 different simulations, we found that three factors relate to the occurrence of artifacts: (1) the magnitude; (2) timing (with relation to data acquisition); and (3) direction of motion.

Our study indicates that minor degrees of motion, such as one pixel, are not sufficient to cause a significant defect by either visual or quantitative analysis. When the MOPA index was under 21, significant visual defects were not observed. The same cut-point was observed for the results of quantitative analysis. Motion was further classified according to different patterns, including shift, bounce, timing of motion and direction. Shifts of one pixel did not produce significant perfusion abnormalities. Bounce also generally did not result in significant perfusion abnormalities, unless occurring in midacquisition. Shifts of two or more pixels were capable of producing defects, but this depended on a second factor: the timing of shift. Motion occurring at midacquisition clearly had the worse effects on visual and quantitative scores. This may be related to the fact that these projections contain the maximum myocardial counts and thus contribute most toward the reconstructed image. Motion occurring at the end of acquisition had the least effect. Downward motion was highly associated with the occurrence of anteroseptal defects and upward motion was associated with the occurrence of anterolateral defects. Inferior wall defects could be produced by either upward or downward motion and were usually associated with midacquisition motion concomitant with pixel deviations ≥2. Inferior wall defects were also observed in the cases of multiple bounces. Besides the production of perfusion defects, significant motion sometimes resulted in recognizable artifacts on thallium scintigraphy. These included the tailing of activity into the background, dislocation and distortion of slices.

TABLE 3
Frequency and Type of Motion in 164 Patients with a Low Likelihood of Coronary Artery Disease

Motion	No.	Abnormal due to motion
Bounce	23 (14%)	0
Upward creep	8 (5%)	0
Multiple bounces	3 (2%)	3
Downward	6 (4%)	3
Upward	1 (0.6%)	1
Lateral	1 (0.6%)	0
Total with motion	42 (26%)	
Total abnormal due to motion		7 (4%)

TABLE 4
Motion Type, Predicted Defects and Actual Defects in 16 Studies With Significant Motion

Motion	Study type	Predicted defects	Actual defects	Group
1	DW	AS	AS, INF	<5% L
2	MB	INF	INF	<5% L
3	MB	INF	INF, HS	<5% L
4	DW	AS	MILD AS	<5% L
5	DW	AS	MILD AS	<5% L
6	MB	INF	INF	<5% L
7	UP	AL, INF	AL, INF	<5% L
8	UP	AL, INF	AL, INF	Mild CAD
9	DW	AS	AS	CABG, LLI
10	DW	AS, INF	AS, INF	NCA
11	UP	AL, INF	AL, INF	40% L
12	MB	INF	Normal	<10% L
13	MB	INF	INF	NCA
14	B*	INF	INF	<10% L
15	DW	AS	AS	NCA
16	B	INF	Normal	NCA

*The bounce occurred at midacquisition.

AL = Antero-lateral defect; AS = antero-septal defect; B = Bounce; CABG = coronary artery bypass surgery; DW = Downward motion; HS = hot spot; IW = inferior; L = likelihood of coronary artery disease; LLI = low likelihood of exercise induced ischemia. MB = multiple bounces; NCA = normal coronary arteries; UP = upward motion.

A hot spot pattern was rarely observed, but was only associated with severe motion. We also assessed lateral motion, but not as thoroughly as for vertical motion, since we found it rarely occurring in the clinical setting. The concavity and narrowness of the imaging table may have helped to reduce the potential for such lateral motion. The movie display of cardiac motion, rather than the added static images, should be used to assess lateral motion.

Previous Studies

Two prior investigations have yielded markedly discordant conclusions concerning the effect of mild simulated

patient motion on scintigraphic studies. In their simulation study of patient motion, Eisner et al. reported that a shift of one pixel in midacquisition produced a 40% false-positive rate for quantitative thallium analysis of SPECT studies (*9*). By contrast, Cooper et al. reported that such simulated patient motion resulted in a false-positive rate of <5% (*10*). Both studies focused on the quantitative analysis of thallium SPECT and differences in their approaches to quantitative analysis may help explain their discordant results. In contrast, our study focused on both the visual and quantitative analysis of thallium scintigraphy, analyzed separately. Our visually and quantitative results, which were highly concordant, are consistent with those observed by Cooper et al., i.e., "mild" motion (e.g., one-pixel shift) was an infrequent cause of false-positive scintigraphic findings in our study.

To evaluate the clinical relevance of our motion simulations, we assessed nine retrospective clinical studies in which significant motion had been identified. From our normal patient population, we identified seven additional patients with significant motion. The patterns of motion in these 16 patients were compared with the patterns created by our motion simulation. The clinical studies corresponded to the scintigraphic pattern noted with similar motion simulation patterns, confirming a predictive relationship between the pattern of motion and the resultant pattern of scintigraphic artifacts. We found also that the various patterns suggestive of motion were relatively specific since a pattern suggestive of motion was observed in only one of 122 patients with a low likelihood of coronary artery disease and no detectable motion.

Patient Motion and False-Positive Rate in Normals

Patient motion was frequent, occurring in 26% of the studies acquired in our low likelihood population. However, the magnitude of patient motion was generally mild, below the threshold deemed to be significant by our simulation study. The most frequent motion patterns were bounce and upward creep. Among the overall normal population, only seven (4%) patients were found to have a false-positive scintigraphic pattern that could be attributed to motion which is lower than we previously reported (*1,2*). This reduction reflects progress made in circumventing the causes of motion artifacts. For instance, we currently begin tomographic imaging 15 min after exercise, to reduce the frequency of upward creep associated with early postexercise hyperventilation (*2*). The initial period between 6–15 min is used to obtain a planar anterior view, important for assessing the presence of transient ischemic dilatation and abnormal pulmonary ^{201}Tl uptake. We instruct the patients to avoid speaking and to stay still during the period of acquisition. Finally, we have designed arm holders which help the patient to stay still during the entire acquisition. Straps may also be used to anchor the patient. Other options for reducing patient motion include the use of point sources and the use of an external light source relative to patient landmark(s), with re-acquisition of a study if gross patient motion is noted during data acquisition.

Motion Correction

Several investigators have developed computer software aimed at detecting and correcting for motion for ^{201}Tl SPECT studies (*9,11*). In our laboratory, we use a simple correction method in which the operator visually identifies the type of motion and manually relocates the frames. Our study provides guidance for motion correction in the clinical setting: for instance, we currently do not correct for motion of one pixel, or for motion occurring in the last frames.

Clinical Implications

Although this study did not assess all types of motion (for instance we did not simulate rotation of frames, since we found it rare in the clinical setting) it helps to understand the mechanisms of motion artifacts. By performing this study, we improved our confidence in detecting motion, interpreting studies with motion and correcting for motion.

ACKNOWLEDGMENTS

The authors would like to thank Dalilah Bellil, MD, for technical assistance, Diane Wayne and Astrid P. Gonzalez for typing the manuscript and Rosa Goldsmith for preparation of the figures. Presented in part at the National Meeting of the Society of Nuclear Medicine, Washington, DC, June 1990. Supported in part by NIH SCOR Grant 17651.

REFERENCES

1. Friedman J, Berman D, Van Train K, et al. Patient motion in thallium-201 SPECT imaging: an easily identified source of artifactual defect. *Clin Nucl Med* 1988;13:5:321–324.
2. Friedman J, Van Train K, Maddahi J, et al. Upward creep of the heart: a frequent source of false-positive reversible defects during thallium-201 stress-redistribution SPECT. *J Nucl Med* 1989;30:1718–1722.
3. DePuey EG, Garcia EV. Optimal specificity of thallium-201 SPECT through recognition of imaging artifacts. *J Nucl Med* 1989;30:441–449.
4. Diamond G, Forrester J. Analysis of probability as an aid in the diagnosis of coronary artery disease. *N Engl J Med* 1979;300:1350–1358.
5. Maddahi J, Van Train K, Prigent F, et al. Quantitative SPECT for detection and localization of coronary artery disease: optimization and prospective validation of a new technique. *J Am Coll Cardiol* 1989;14:689–699.
6. Fintel D, Links J, Binker J, Frank T, Becker L. Improved diagnostic performance of exercise thallium-201 single photon emission computerized tomography over planar imaging in the diagnosis of coronary artery disease: a receiver operating characteristic analysis. *J Am Coll Cardiol* 1989;13:600–612.
7. Port S, Oshima M, Ray G, et al. Assessment of single vessel coronary artery disease: results of exercise electrocardiography, thallium-201 myocardial perfusion imaging and radionuclide angiography. *J Am Coll Cardiol* 1985; 6:75–83.
8. Maddahi J, Van Train K, Wong C, et al. Comparison of thallium-201 single photon emission computerized tomography (SPECT) and planar imaging for evaluation of coronary artery disease [Abstract]. *J Nucl Med* 1986;27:999.
9. Eisner R, Churchwell A, Noever T, et al. Quantitative analysis of the tomographic thallium-201 myocardial bullseye display. Critical role of correction for patient motion. *J Nucl Med* 1988;29:91–97.
10. Cooper JA, Newman PH, McCandless BK. Effect of patient motion on tomographic myocardial perfusion imaging. *J Nucl Med* 1992;33:1566–1571.
11. Geckle W, Franck T, Links J, Becker L. Correction for patient and organ movement in SPECT: application to exercise thallium-201 cardiac imaging. *J Nucl Med* 1988;29:441–450.